ELSEVIER

Thermochimica Acta 249 (1995) 335–349

thermochimica acta

Thermal and water vapor effects on the rate of the dehydration reactions of barium chloride

Janice Antoine Lumpkin*[,1], Daniel D. Perlmutter

Department of Chemical Engineering, University of Pennsylvania, Philadelphia, PA 19104-6393, USA

Received 30 July 1993; accepted 5 June 1994

Abstract

The dehydration kinetics of barium chloride dihydrate to the monohydrate and/or anhydrous salt were found to be very sensitive to the temperature, bulk water-vapor pressure, and sample and particle sizes. Dehydrations were conducted isothermally between 317 and 333 K under either moderate vacuum or water vapor atmospheres ranging from 40 to 6.67×10^2 Pa. Particle sizes ranged between 53 and 710 μm. Activation energies were found to vary with sample size and extent of conversion; apparent values ranging from 92 to 150 kJ mol^{-1} were measured. Enthalpy of reaction estimates also varied with sample size and temperature; values ranging from 115.9 to 137.2 kJ mol^{-1} were obtained.

The sensitivities to the temperature, water vapor pressure, sample and particle size were found to be significantly affected by transient changes in local water vapor pressure caused by inter- and intraparticle diffusional limitations. Possible mechanistic changes with changing water vapor pressure are discussed. Transient increases in water vapor pressure in the interior of large particles caused crystallization of the monohydrate under conditions where it did not otherwise form.

Keywords: Barium chloride; Calorimetry; Dehydration; Kinetics; TGA

1. Introduction

The thermal decomposition–recombination kinetics of fully reversible gas–solid reactions has gained interest because of potential application in chemical heat pump

* Corresponding author.

[1] Present address: Department of Chemical and Biochemical Engineering, University of Maryland Baltimore County, Baltimore, MD 21228, USA.

SSDI 0040-6031(94)01929-0

systems employing intermittent absorption cycles [1–4]. Previous studies of inorganic salt hydrates have focused primarily on irreversible dehydration reactions; a few more recent studies have included mathematical models of reversible reactions [5,6] and diffusion [6,7]. Enthalpies of reaction and activation energies are often scattered and depend on the reaction configuration employed, the history of the samples used [8] and/or the extent of reaction [9].

Water vapor is known to have complex effects on thermal dehydration behavior. The dehydration rate, intermediate structures, and the crystallinity of the product phase all can vary with changes in water vapor pressure [10–14]. Reaction rates do not always decrease monotonically with increasing pressure [10,15–17] and reaction rates can approach zero far from equilibrium [18]. The former non-monotonic pressure dependence (the Smith–Topley effect) is largely attributed to the opposing effects of water acting both as an inhibitor, through the reverse reaction, and a promoter, through the crystallization of the product phase, of the dehydration reaction [12]. The role of water vapor is further complicated by unknown diffusion and readsorption rates of the vapor through the product phase. The wide variety of reaction–product interfaces observed for different compounds [9,19] brings additional complexity to this analysis.

Practical use of salt hydrates involves operation under varying temperature and water vapor pressure conditions; therefore, thermal parameters and effects of transient changes in water vapor pressure are expected to be important. This research addresses the effect of temperature, water vapor partial pressure, and particle size on the dehydration kinetics of the fully reversible reactions of the barium chloride–water system. Structural changes in the solids were determined as a function of conversion.

2. Background

The $BaCl_2$–H_2O system is one of the few hydrates that has been demonstrated to undergo fully reversible dehydration–rehydration reactions [2]. The di- and monohydrate are the most commonly reported hydrates [8,20–24]; however, a hemihydrate has also been documented [25–27]. The possible reactions have been reviewed recently [7]. The dihydrate to monohydrate, and monohydrate to anhydrous salt reactions are commonly observed to proceed in a stepwise manner; however, under moderate vacuum conditions the reactions overlap and the dihydrate reacts directly to form the anhydrous salt [7]. Wendlandt and Simmons [28] noted for non-isothermal dehydrations of the dihydrate that the first water loss was more clearly separated from the second water loss in water saturated atmospheres versus dry atmospheres. Water vapor partial pressure [2,3,29] and the number of previous reaction cycles [2] have been shown to be important variables which affect both the dehydration and rehydration rates. Ingraham and Rigaud [22] reported that the dehydration rate of dihydrate pellets to the monohydrate decreased monotonically but non-linearly with increasing water vapor pressure. They interpreted the curvature of the dehydration rate–water vapor driving force curve as an

Table 1
Enthalpy of reaction data (in kJ mol^{-1}) for dehydrations of hydrated barium chloride [a]

Dihydrate→ monohydrate	Monohydrate→ anhydrous salt	Dihydrate→ anhydrous salt	Ref.
61.04 ± 0.84	–	–	[21]
58.20 ± 0.04	58.62 ± 0.04	116.8 ± 1.8 [b]	[24]
–	–	118.3 [c]	[24]
50.5 ± 3.3	55.2 ± 3.3	–	[20]
61.9	56.5	–	[31]
–	57.7	–	[33]
69.9 ± 2.9	79.49 ± 5.4	–	[8]
50.21	–	–	[32]
59.4 ± 10.5	75.7 ± 3.3		[30]

[a] All results are listed exactly as reported by the investigators referenced. [b] Sum of dihydrate and monohydrate dehydrations. [c] Calculated from ΔH_f° values at 25°C.

indication that the reaction rate was influenced by adsorption of water to the product interface.

Enthalpy of reaction data for the dehydration reactions have been reported by several investigators [8,20,21,24,30–33]; the results are as listed in Table 1. Arrhenius data have been determined for powders [20,21,24], pellets [22] and single crystals [23]. In general it is found that barium chloride dihydrate belongs to the class of "abnormal" compounds which have anomalously large activation energies and pre-exponential factors [23]. A summary of several representative activation energies and pre-exponential factors for dehydration of the powders is listed in Table 2. Some differences are found between isothermal and non-isothermal studies which have mechanistic implications.

Based on their interpretation of their experimentally determined isothermal and non-isothermal activation energies, Ingraham and Rigaud [22] postulated that the dihydrate to monohydrate and monohydrate to anhydrous dehydrations proceed through amorphous intermediates which must undergo an exothermic transition to the crystalline lower hydrate. Under isothermal conditions they report that the decomposition and recrystallization reactions overlap, whereas under non-isothermal conditions there is a lag between these processes. They note that low temperature dehydrations and dehydrations conducted under high vacuum conditions favor the separation of the processes. The enthalpy changes for the transitions of the monohydrate and the anhydrous salt were estimated to be $\approx$10.5 and $\approx$33.5 kJ mol^{-1}, respectively.

Activation energies can vary as a function of conversion for reversible dehydration/rehydration reactions [9]; however, such data have not been reported for barium chloride. Galwey et al. [9] reported activation energies which increased with increasing extent of conversion in their studies of lithium sulphate monohydrate. They attributed this to a reduction of the forward reaction rate by an increase in the reverse reaction rate caused by increased water vapor. These reactions were con-

Table 2
Activation energies and pre-exponential factors for barium chloride dehydrations

Dihydrate→ monohydrate		Monohydrate→ anhydrous		Method and model
E_{act}/kJ mol^{-1}	log(A/s^{-1})	E_{act}/kJ mol^{-1}	log(A/s^{-1})	
111.7 ± 1.0	14.28 ± 0.15	79.9 ± 1.4	8.29 ± 0.20	Powder isothermal TGA, R_n [a] [21]
110.5 ± 0.8	14.27 ± 0.13	80.0 ± 1.0	8.17 ± 0.15	Powder isothermal TGA, A_m [b] [21]
78.7 ± 5.0	–	≈41.8 [c]	–	Powder isothermal DSC, A_2 [b]
		69.0 ± 4.6 [d]		[20]
94.5 ± 5.4	–	102.5 ± 6.3 [c]	–	Powder non-isothermal DSC,
		90.8 ± 4.6 [d]		R_2 [a][20]
64.4 ± 9.6	–	67.8 ± 12.5 [c]	–	Powder pellet isothermal
		71.5 ± 7.1 [d]	–	conductivity [22]
75.3 ± 5.0	–	111.3 ± 7.1 [c]	–	Powder pellet non-isothermal
		95.4 ± 16.7 [d]	–	conductivity [e] [22]
79.5 ± 9.2	–	111.7 ± 15.1 [c]	–	Powder pellet non-isothermal
		101.7 ± 18.4 [d]	–	conductivity [f] [22]

[a] R_n represents phase boundary or shrinking core model for conversion (α) which is given by the expression $1-(1-\alpha)^{1/n}=kt$. [b] A_m represents the Avrami–Erofe'ev model for conversion which is given by the expression $[-\ln(1-\alpha)]^{1/m}=kt$. [c] Monohydrade from dihydrate. [d] Fresh monohydrate. [e] Mean value from experiments done without water vapor back pressure. [f] Mean value from experiments done with and without water vapor back pressure (pressure range 20–2.35 × 10^2 kPa).

ducted under closed conditions in which the evolved water vapor remained in the reaction vessel.

The crystallinity and porosity of the reactive intermediates can affect both the dehydration and rehydration rate. Osterheld and Bloom [23] studied the dehydration nuclei and reaction interface of the barium chloride dihydrate (single crystals) to monohydrate reaction. They reported that cracking occurred in the monohydrate product but that no cracking could be observed at the reaction interface. They proposed that the dehydration proceeds through a transition state where the dehydrate structure is retained with half of its water molecules removed. Since crack formation is attributed to the formation of the monohydrate lattice which has a molar volume that is 12% less than the dihydrate, cracking would not be expected to occur until the monohydrate phase had crystallized.

Galwey and Mohamed [34] reached similar conclusions in their studies of the reaction interfaces of the alums $KAl(SO_4)_2 \cdot 2H_2O$ and $KCr(SO_4)_2 \cdot 12H_2O$. Specifically they concluded that the initial reactant–product interface is coherent, that the retention of water vapor in the dehydration nuclei which make up this interface promote the recrystallization of the product, and that cracking occurs just beyond the immediate reaction zone. Andersson et al. [2] reported that a network of cracks and pores were formed when the dihydrate–monohydrate dehydration/rehydration

reactions were performed several times; however, the particles retained their overall shape.

Slow or incomplete transformation of the crystalline product has been postulated by several investigators [20,35]. In comparing the X-ray diffraction patterns generated by monohydrate produced by dehydration from the dihydrate versus monohydrate which had been crystallized in solution, Guarini and Spinicci [20] noted that the former "did not attain a perfect crystallinity".

Water vapor has been shown to affect the crystalline state of the intermediates and dehydration products of several salt hydrates including copper, zinc and magnesium sulphate hydrates [36–38]. Frost et al. [36] and Quinn et al. [37] showed that the copper hydrates formed an amorphous monohydrate which continued to crystallize long after the water molecules had been removed to the crystalline monohydrate product. These metastable amorphous intermediates formed under vacuum or low water vapor pressure conditions. No long-lived amorphous intermediate was formed above a critical pressure of about 133–267 Pa. Other investigators have reported stoichiometric and non-stoichiometric metastable intermediates far from equilibrium. Andersson and Azoulay [39] observed this in non-isothermal, constant water vapor pressure dehydrations of $Na_2S \cdot H_2O$; Lallemant and Watelle-Marion [40] reported that $MgSO_4 \cdot 4H_2O$ and $MgCrO_4 \cdot 5H_2O$ formed metastable intermediates under certain water vapor pressure and temperature combinations.

3. Experimental apparatus and procedures

3.1. Materials

Reagent grade crystalline powders of barium chloride dihydrate were used in each analysis. The TGA studies were conducted with Baker barium chloride sieved to standard size fractions ranging from 5.3×10^{-3} to 7.1×10^{-2} cm (53–710 μm); the calorimetry, SEM, gas adsorption and mercury porosimetry studies were conducted with EM Science barium chloride sieved to standard size fractions ranging from 7.5×10^{-3} to 1.5×10^{-2} cm (75–150 μm).

3.2. Thermogravimetric analysis

The dehydration kinetics were monitored on a Cahn 2000 Recording Electrobalance Thermogravimetric Analyzer (TGA). A Welch Duo-Seal vacuum pump and a water vapor delivery system were added to the TGA unit to allow vacuum dehydrations and dehydrations under static water vapor atmospheres. The vacuum pump was capable of maintaining a vacuum of ≈ 10 Pa. The pressure was monitored with a Serta electronic manometer.

The water vapor pressure was controlled by connecting the TGA assembly to a flask containing distilled water or a saturated solution of calcium chloride hexahydrate. The assembly was evacuated and purged five times with water vapor at 1.6×10^3 to 2.0×10^3 Pa prior to each run. The sample was then heated slowly and

allowed to come to thermal equilibrium ($\approx$1 h) under the water vapor atmosphere. The dihydrate was stable at this pressure for the temperature range of interest. During this time the water bath temperature was adjusted to the appropriate temperature and allowed to equilibrate. Dehydration was initiated by applying a vacuum until the first sign of water loss was detected ($\approx$9 min). After initiation, the vacuum source was disconnected and the system was exposed to the water vapor delivery system. This procedure was used to bypass the long induction period commonly observed in dehydration reactions.

3.3. Calorimetry

Dehydration experiments were performed in a Seteram C-80 twin-cell heat-flux calorimeter from which simultaneous kinetic and enthalpy of reaction data were collected. All experiments were conducted under isothermal conditions. Both sample and reference cells were connected to a Hause-Leobold vacuum pump via flexible metal hosing. A Sargent-Welch model 1516 electronic thermocouple vacuum gauge that measures pressure in the range of $0-6.67 \times 10^2$ Pa was mounted between the cells. The minimum pressure obtained experimentally was 17.3 Pa.

3.4. X-ray diffraction

X-ray analyses were performed on a Rigaku Rotaflex Diffractometer, using copper Kα radiation. A thin layer of sample powder was mounted on a glass microscope slide. The X-ray source was a 12 kW rotating anode.

3.5. Gas adsorption and porosimetry

Nitrogen and krypton adsorption isotherms were measured on a Quantachrome Quantasorb Sorption System. Surface area measurements of the barium chloride dihydrate starting material were made with Kr because the surface areas were too low to give accurate N_2 measurements. Approximately 2 g of material was required to obtain reproducible results. Surface area measurements of reaction intermediates and products were made with N_2. Samples of intermediate conversion were obtained by quenching the reaction with liquid nitrogen. A Quantachrome Autoscan-60 Mercury Porosimeter was used to collect pore volume data for pore radii ranging between 1.8×10^{-3} and 1 μm.

4. Results and discussion

4.1. Temperature dependency

Conversion data were collected at different temperatures and for several sample sizes in order to assess the impact of diffusion and transient increases in water vapor pressure on thermal parameters. Experiments conducted at 318, 326 and 333 K under

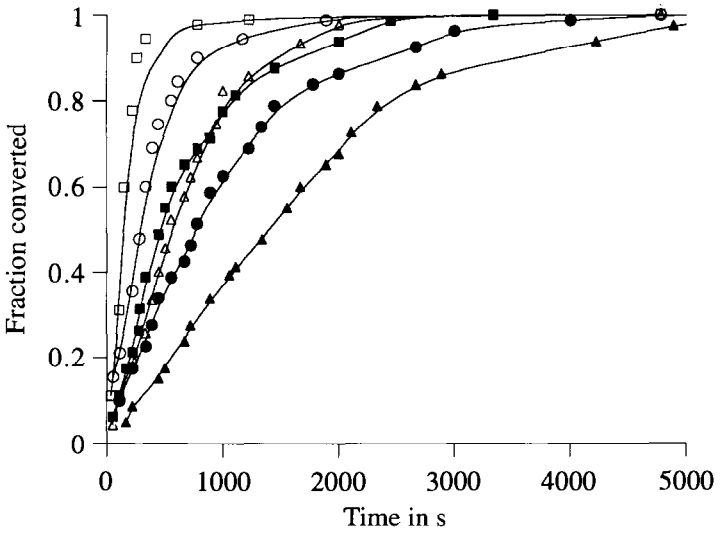

Fig. 1. Effect of temperature on dehydration under vacuum for 11 and 223 mg samples: □, 333 K; ○, 326 K; △, 318 K; ■, 333 K; ●, 326 K; ▲, 318 K.

a moderate vacuum showed that the dehydration rate increased with increasing temperature for all sample sizes. The conversions for three sample sizes (11, 223 and 1607 mg) are shown in Figs. 1 and 2. The smaller dihydrate samples appear to dehydrate directly to the anhydrous salt with a nearly simultaneous loss of the two waters of hydration (Fig. 1). For the larger sample sizes, the water loss proceeded in a stepwise manner and produced the sharp "knee" in the conversion with respect to time for the two lower temperatures (Fig. 2). At 333 K, the large-sized sample exhibited a slight bend in conversion with respect to time and appears to dehydrate in one step.

Arrhenius parameters for a small (11 mg) and large (1607 mg) sample are listed in Table 3; the data were analyzed as a two-step process. The activation energies of the first and second step for the smaller sample (113.8 and 150.6 kJ mol^{-1}, respectively) are greater than for the larger sample (93.7 and 128.0 kJ mol^{-1}, respectively). The result for the 11 mg sample size, stage I dehydration, is in good agreement with the isothermal results reported by Tanaka [21] for the dihydrate–monohydrate reaction. The result for the larger particle size agrees with other reported isothermal and non-isothermal powder data (see Table 2).

The lack of agreement between the Arrhenius parameters determined from the small- and large-sized sample dehydrations cannot be attributed simply to typical diffusional falsification of kinetics which predicts a decrease in apparent activation energy for isothermal reactions due to the diffusional resistances [41]. The Arrhenius data also reflect differences in the dehydration mechanisms, caused by transient changes in the water vapor environment. The water vapor pressure over the sample bed was measured throughout the course of these reactions and were reported previously [7]. Maximum transient pressures above the small- and large-sized

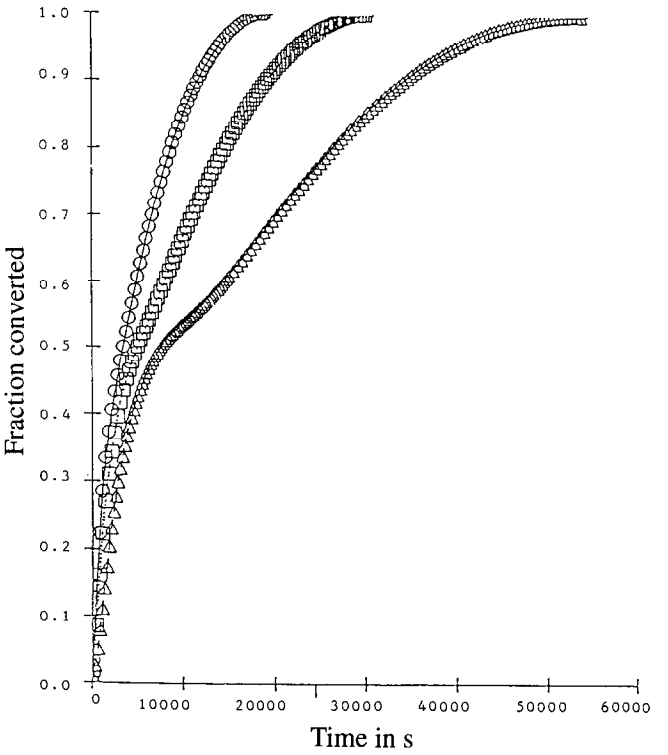

Fig. 2. Effect of temperature on dehydration under vacuum for 1607 mg samples: ○, 333 K; □, 326 K; △, 318 K.

Table 3
Arrhenius parameters

Sample size/mg	Stage I			Stage II		
	E_{act}/kJ mol^{-1}	A/s^{-1}	r^2	E_{act}/kJ mol^{-1}	A/s^{-1}	r^2
11	113.8	2.04×10^{15}	0.995	150.6	2.58×10^{20}	0.993
1609	93.7	2.68×10^{8}	0.996	128.0	1.49×10^{12}	0.999

particles were 38.7 and 105.3 Pa, respectively, at 318 K; and 67.3 and 160.0 Pa, respectively, at 333 K.

X-ray analyses done at several intermediate conversions showed that the small sample size dehydration reactions did not proceed through a crystalline monohydrate intermediate, while the large sample dehydrations did [7]. Therefore, stage I of a small sample dehydration reaction refers to the loss of the first water molecule from the dihydrate to form a skeleton of the dihydrate with one water molecule missing, an X-ray amorphous monohydrate structure, or some other intermediate

structure. In contrast, stage I of a large sample dehydration reaction refers to the loss of the first water molecule to form the crystalline monohydrate.

Thus in addition to diffusional effects, the difference in activation energies between the large and small samples includes the energy difference of a transition from an intermediate to a crystalline monohydrate. Since this recrystallization occurs during the dehydration of the large-sized samples, the endothermic decomposition and exothermic recrystallization processes overlap. The energy difference is ≈ 20 kJ mol^{-1}, which is consistent with the findings of Ingraham and Rigaud [22].

Stage II of the dehydration reaction for the small samples represents the transition to an anhydrous salt. The activation energy for the small samples is ≈ 23 kJ mol^{-1} larger than that of the large sample. If an analogous situation exists between the first and second stages of the reaction, an X-ray amorphous anhydrous intermediate or the monohydrate skeleton with the water vapor removed may be possible intermediates.

The large difference in dehydration kinetics resulting from different structural intermediates is consistent with the findings of Gaponov et al. [42] who reported that the isothermal decomposition kinetics of inorganic salt hydrates were controlled by structural reorganization of metastable intermediates to the final product, as opposed to the release of water vapor. Although this work was done with two different hydrates (with equivalent water molecule sub-lattices), the analysis is expected to apply to the same hydrate dehydrating by different mechanisms.

For both the small- and large-sized samples, the second step is more temperature-sensitive than the first and, correspondingly, the activation energy for the second step is higher than the first. This difference could be attributed to the increased importance of the reverse reaction. The discrepancies between these activation energies and those of the reported literature can be attributed to these complex diffusional effects.

4.2. Water vapor effects

The effect of a sustained water vapor environment was studied for bulk water vapor pressures ranging from 42.3 to 663 Pa. All dehydrations were performed on the TGA at 317 K. The conversions for water vapor pressures of 42.3 to 124 Pa show (Fig. 3) that the dehydration rate decreases with increasing water vapor pressure, as expected for a reversible reaction. Above 160 Pa, severe reductions in the reaction rate were observed (fractional conversion <0.0002/h) at several intermediate conversions in addition to the decrease in the initial reaction rate. In the pressure range of 163 to 175 Pa, the reaction slowed at fractional conversions ranging from 0.52 to 0.70, as illustrated in Figs. 3 and 4. Above 180 Pa, fractional conversions of 0.48 and less were observed, as shown in Fig. 4.

The reported vapor pressure data show that the dihydrate–monohydrate equilibrium pressure is between 1600 and 3600 Pa and the monohydrate–anhydrous salt equilibrium is between 93.3 and 1600 Torr at 317 K [22,30–32,43,44]. The dihydrate–monohydrate equilibrium pressure is well above the pressure range tested; however, the monohydrate–anhydrous equilibrium pressure may lie within

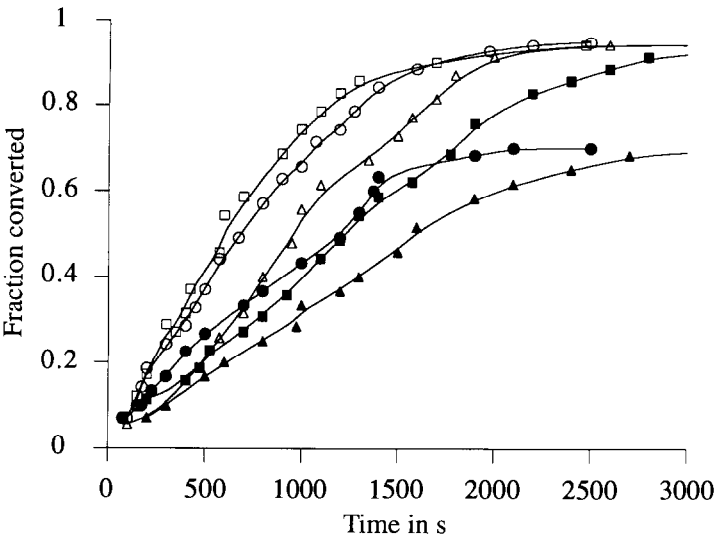

Fig. 3. Effect of water vapor pressure on dehydration kinetics at 317 K; vacuum to 164 Pa: □, vacuum; ○, 42.3 ± 0.9 Pa; △, 89.9 ± 0.3 Pa; ■, 124 ± 0.4 Pa; ●, 163 ± 0.7 Pa; ▲, 164 ± 1.3 Pa.

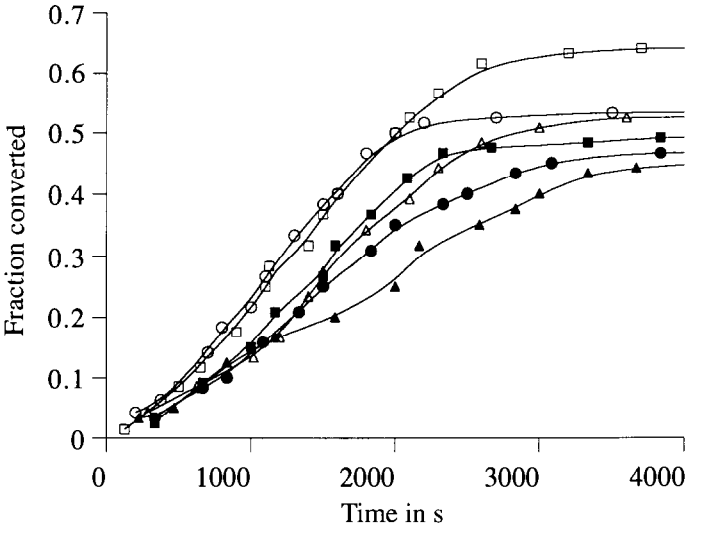

Fig. 4. Effect of water vapor pressure on dehydration kinetics at 317 K; 167–663 Pa: □, 167 ± 0.7 Pa; ○, 171 ± 1.3 Pa; △, 175 ± 1.3 Pa; ■, 193 ± 1.3 Pa; ●, 225 ± 5.3 Pa; ▲, 663 ± 2.7 Pa.

this range though the exact point is uncertain. Fig. 3 shows that complete dehydration occurs at 124 Pa so that the monohydrate–anhydrous equilibrium cannot be as low as 93.3 Pa. As previously mentioned, barium chloride dihydrate has been reported to dehydrate in a stepwise manner via the crystalline monohydrate;

therefore, equilibrium data for the dihydrate–anhydrous salt system have not been reported.

Several explanations for the severe rate reductions at the higher water vapor pressures are possible.

(1) The slow reaction rates are caused by being at or near the dihydrate–anhydrous salt equilibrium pressure so that the incomplete conversions correspond to equilibrium mixtures of the dihydrate and anhydrous salt.

(2) The slow reaction rates are caused by being at or near the monohydrate–anhydrous salt equilibrium pressure so that the non-stoichiometric solids are equilibrium mixtures of the monohydrate and anhydrous salt.

(3) The slow reaction rates are caused by the formation of a metastable intermediate far from equilibrium which might be a mixture of any of the solids.

A likely explanation for the abrupt change in kinetic behavior in the narrow pressure range of 124–163 Pa is that the monohydrate (or a lower hydrate) was formed in the interior of the particle and subsequently dehydrated at a lower rate. This hypothesis is based on the previous finding that severe decreases in reaction rates occur when larger sample beds of barium chloride dihydrate were dehydrated under moderate vacuum conditions [7]. In these studies, transient increases in water vapor pressure, caused by slow diffusion of water vapor through the bed of barium chloride powder, were monitored over the course of the dehydration reaction. For sample beds of 250 μm and larger, the transients were of the order of 80 Pa for a total pressure of 97.3 Pa above the sample bed and higher within the bed. This resulted in the formation of the crystalline monohydrate as an intermediate, whereas dehydrations of more shallow beds of particles under identical conditions did not result in monohydrate formation.

Under conditions where the monohydrate formed, severe reductions in reaction rate persisted over the course of the reaction, even though the reactions were conducted under moderate vacuum. In the most extreme case (at 318 K), the time required for complete dehydration increased from approximately 17 min to 16 h. Thus an explanation of the severe reduction in reaction rates in the constant water vapor studies is that the monohydrate crystal was formed in the interior of the particle as a result of intraparticle transient increases of the water vapor pressure. Once formed, the monohydrate continues to dehydrate at a very slow rate compared to the starting material. In the constant pressure runs of 171 Pa and above, the weight of the metastable intermediate corresponds to the monohydrate. When the water vapor pressure is between 163 and 167 Pa the water content of the intermediate ranges from 30 to 45% of the initial water content and the solid is probably a mixture of the monohydrate and anhydrous salt. The formation of the hemihydrate cannot be ruled out at this time.

4.3. Effects of particle size and structural changes

Particle size studies were conducted to test the hypothesis concerning formation of one or more lower hydrates in the interior of the particles. If the monohydrate (or other lower hydrate) can crystallize in the interior of a particle, one would

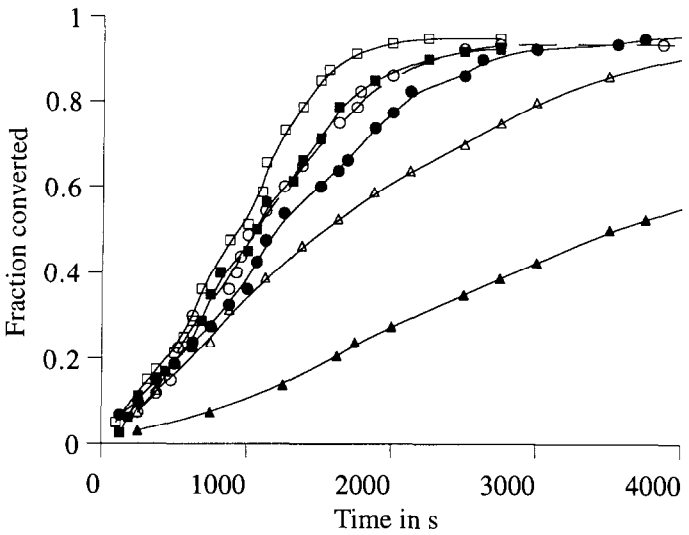

Fig. 5. Effect of particle size on dehydration kinetics at 317 K; 84.0–128 Pa: □, 53–63 μm; ○, 212–250 μm; △, 600–710 μm; ■, 53–63 μm; ●, 212–250 μm; ▲, 600–710 μm.

expect that the abrupt decrease in fractional conversion would be observed at lower water vapor partial pressures for larger particles. Dehydrations were conducted with 10 mg samples at the particle size used in all of the preceding experiments, 53–63 μm, and at two additional larger particle sizes, 212–250 μm and 600–710 μm, under controlled water vapor atmospheres ranging from 84.0 to 172 Pa. The results are presented in Figs. 5 and 6, supplementing the results for the same

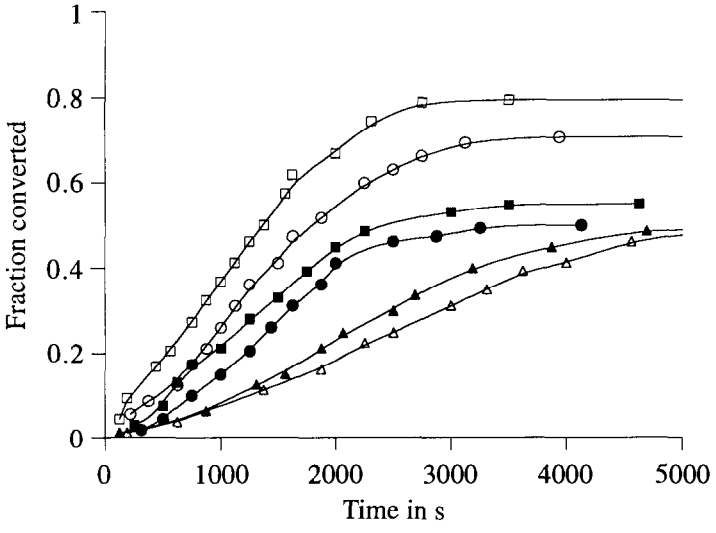

Fig. 6. Effect of particle size on dehydration kinetics at 317 K; 161–172 Pa: □, 53–63 μm; ○, 212–250 μm; △, 600–710 μm; ■, 53–63 μm; ●, 212–250 μm; ▲, 600–710 μm.

particles under vacuum conditions that were reported earlier [7]. As expected, two observations were made for increasing particle size: (1) the overall dehydration rate decreased and (2) the water vapor pressure decreased, when severe reductions in the dehydration rate were observed.

Since this explanatory scheme requires that the water vapor pressure in the interior of the particle exceeds the ambient pressure, structural analyses were conducted to further assess the feasibility of this reaction pathway. Mercury porosimetry, gas adsorption and SEM measurements showed that the particles develop a slit-like pore structure upon dehydration; however, surface area measurements of the monohydrate intermediate and the anhydrous product showed them both to be relatively low porosity materials (1.7 ± 0.6 and 3.8 ± 0.8 m^2 g^{-1}, respectively) [45].

It is also possible that the cracking observed in the reaction product and intermediate does not occur in the dehydration nuclei during dehydration. In that event, the non-porous nature of the starting material ($9.3 \times 10^{-2} \pm 4.2 \times 10^{-2}$ $m^2 g^{-1}$) is retained upon initial removal of the water molecules and a reaction interface exists that could support even higher transient water vapor pressures. This type of interface is consistent with Osterheld amd Bloom's [23] observations for single crystals.

Comparison of the particle size effect with the sample size effect previously reported [7] shows that the critical internal and external diffusion lengths were of the same order of magnitude. Particle size studies under moderate vacuum conditions show that the particle thickness at which the severe reductions in rate occurred is ≈ 250 μm. Because diffusion can occur from either side of the particle (as confirmed by optical microscopy [45]), the effective diffusion length is ≈ 125 μm. In the sample size studies, diffusional losses can only occur from the top of the sample bed; thus the effective diffusion length is the depth of the sample bed. Severe reductions in the reaction rate were observed for sample beds of ≈ 110 μm and greater.

4.4. Enthalpy of reaction

The enthalpy of reaction values varied with the sample size at each of the experimental temperatures, as shown in Table 4. This variation most likely reflects

Table 4
Enthalpy of reaction estimates

Sample size/mg	Enthalpy of reaction/(kJ mol^{-1})		
	318 K	326 K	333 K
11.0 ± 1.0	137.2 ± 10.0	133.9 ± 5.4	122.3 ± 2.4
45.0 ± 2.0	123.7 ± 1.0	120.8 ± 1.5	116.7 ± 1.7
87.5 ± 0.7	119.7 ± 0.2	119.1 ± 1.0	116.6 ± 0.3
227.8 ± 5.3	117.4 ± 0.4	117.0 ± 0.2	116.5 ± 0.2
445.0 ± 2.0	117.7 [a]	116.8 ± 0.5	116.5 ± 0.1
908.0 ± 3.0	116.8 ± 0.2	116.5 ± 0.2	116.3 ± 0.1
1608.5 ± 1.5	115.9 ± 0.9	116.7 [a]	116.6 ± 0.1

[a] One data point.

differences in the crystal structure of the final product. Since increasing sample size and temperature corresponded to increases in the maximum transient bulk water vapor pressure and transient increases in water vapor have been shown to affect the crystal structure of the intermediate, it is possible that the crystalline state of the final product is affected by the water vapor environment present during reaction.

5. Conclusions

The dehydration kinetics of barium chloride dihydrate are very sensitive to both the bulk water vapor pressure and transient changes in the local water vapor environment. These sensitivities arise because of changes in the structure of the reaction intermediates. Water vapor pressure gradients caused by mass transfer resistances through particles of diameters of ≈ 250 μm and larger are sufficient to cause severe changes in the reaction rate. Intrinsic activation energies for the decomposition of barium chloride hydrates can only be determined under conditions where the particle size is below ≈ 50 μm and water vapor removal is rapid and complete. The reaction rate as a function of water vapor partial pressure must be determined under conditions where the bulk water vapor is tightly controlled and transient fluctuations are minimized. Whether such sensitivity to the product vapor pressure is representative of other fully reversible solid decomposition reactions should be investigated in order to expand the basic understanding of the reaction kinetics of this class of compounds and to facilitate their usage in engineering applications.

Acknowledgments

The facilities for the bulk of this work were provided by BP America at the Warrensville Research Center, Warrensville Heights, Ohio. We are particularly grateful to Dr. Jeanette G. Grasselli, Director of Research Science BP America, and Dr. Alex McMaster, Analytical Business Liaison, for their role in arranging access to the facilities. For technical assistance in gas adsorption and porosimetry we thank Tom Bartkowski and Lina Patel; in X-ray diffraction and thermal analysis, we thank Gregory Alexander, Mark Santana, Ernest Armstrong, Martin Mittleman, Dr. Sampath Iyengar and Dr. Phillip Engler.

References

[1] M.A. Stanish and D.D. Perlmutter, Solar Eng., 26 (1981) 333.
[2] J.A. Andersson, M. Azoulay and J. de Pablo, Thermochim. Acta, 70 (1983) 291.
[3] J.A. Andersson, M. Azoulay and J. de Pablo, Int. J. Eng. Res., 12 (1988) 137.
[4] P. O'D. Offenhartz, F.C. Brown, R.W. Mar and R.W. Carling, J. Solar Eng., 102 (1980) 59.
[5] M.A. Stanish and D.D. Perlmutter, AIChE J., 30 (1984) 56.
[6] V.B. Okhotnikov, S.E. Petrov, B.I. Yakobson and N.Z. Lyakhov, React. Solids, 2 (1987) 359.

[7] J.A. Lumpkin and D.D. Perlmutter, Thermochim. Acta, 202 (1992) 151.
[8] M. Rigaud and T.R. Ingraham, Can. Metall. Q., 4(4) (1965) 237.
[9] A.K. Galwey, N. Koga and H. Tanaka, J. Chem. Soc. Faraday Trans., 86(3) (1990) 531.
[10] D.A. Young, Decomposition of Solids, Pergamon Press, Oxford, 1966.
[11] W.E. Garner, Chemistry of the Solid State, Academic Press Inc., London, 1955.
[12] N.Z. Lyakhov and V.V. Boldyrev, Russ. Chem. Rev., 41(11) (1972) 919.
[13] A.I. Zagary, V.V. Zyryanov, N.Z. Lyakhov, A.P. Chupakin and V.V. Boldyrev, Thermochim. Acta, 29 (1979) 115.
[14] R.M. Dell and V.J. Wheeler, Reactivity of Solids, 5th Inter. Symp., Elsevier, New York, 1965.
[15] B. Topely and M.L. Smith, J. Chem. Soc., (1935) 321.
[16] G.B. Frost and R.A. Campbell, Can. J. Chem., 29 (1963) 604.
[17] R.C. Wheeler and G.B. Frost, Can. J. Chem., 33 (1955) 545.
[18] M.A. Stanish and D.D. Perlmutter, AIChE J., 30 (1984) 56.
[19] A.K. Galwey, J. Therm. Anal., 38 (1992) 99.
[20] G.G.T. Guarini and R. Spinicci, J. Therm. Anal., 4 (1972) 435.
[21] H. Tanaka, Thermochim. Acta, 52 (1982) 1.
[22] T.R. Ingraham and M. Rigaud, Can. Metall. Q., 4(4) (1965) 247.
[23] R.K. Osterheld and P.R. Bloom, J. Phys. Chem., 82(14) (1978) 159.
[24] H. Tanaka and K. Maede, Thermochim. Acta, 51 (1981) 97.
[25] J. Kessis, C.R. Acad. Sci., 264C (1967) 973.
[26] V.G. Assarsson, Z. Anorg. Chem., 244 (1940) 330.
[27] JCPDS (Joint Committee on Powder Diffraction Srandards), PDF (Powder Diffraction Files), 1986.
[28] W.W. Wendlandt and E.L. Simmons, Thermochim. Acta, 3 (1972) 171.
[29] J. de Pablo Ribas and M. Azoulay, An. Quim., 83(1) (1987) 23.
[30] E.M. Collins and A.W.C. Menzies, J. Phys. Chem., 40 (1936) 379.
[31] H.W. Foote and S.R Scholes, J. Am. Chem. Soc., 33 (1911) 1309.
[32] G.P. Baxter and W.C Cooper, J. Am. Chem. Soc., 46 (1940) 923.
[33] National Bureau of Standards Tech. Note, No. 270-6, Washington D.C., 1971, p. 81.
[34] A.K. Galwey and M.A. Mohamed, Thermochim. Acta, 121 (1987) 97.
[35] J.L. McAtee, Clays Clay Miner., 18 (1970) 223.
[36] G.B. Frost, K.A. Moon and E.H. Tompkins, Can. J. Chem., 31 (1951) 604.
[37] H.W. Quinn, R.W. Missen and G.B. Frost, Can. J. Chem., 33 (1955) 286.
[38] R.I. Razouk, R.S. Mikhail and H.Y. Ghorab, J. Appl. Chem., 19 (1969) 329.
[39] J.Y. Andersson and M. Azoulay, J. Chem. Soc. Dalton Trans., (1986) 469.
[40] M. Lallemant and G. Watelle-Marion, C.R. Acad. Sci., Ser. C, 272 (1971) 139.
[41] H.S. Fogler, Elements of Chemical Reaction Engineering, 2nd ed., Prentice-Hall, Englewood Cliffs, NJ, 1992.
[42] Y.A. Gaponov, B.I. Kidyarov, N.A. Kirdyashkina, N.Z. Lyakhov and V.B. Okhotnikov, J. Therm. Anal., 33 (1988) 547.
[43] J.R. Partington, J. Chem. Soc., 99 (1911) 466.
[44] M.A. Stanish, Hydration–dehydration kinetics of inorganic salts with potential heat pump applications, Ph.D. Thesis, University of Pennsylvania, 1982.
[45] J.A. Lumpkin, Kinetics of the dehydration reactions of hydrated barium chloride, Ph.D. Thesis, University of Pennsylvania, 1988.